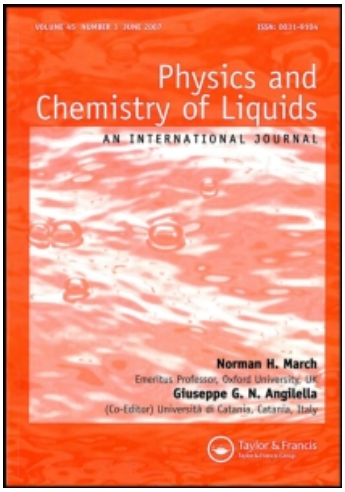

Physics and Chemistry of Liquids
Publication details, including instructions for authors and subscription information:
http://www.informaworld.com/smpp/title~content=t713646857

The structure changes in $Sn_{1-x}Ti_x$ alloys at transition from liquid to solid state

S. Mudry[a]; A. Korolyshyn[a]; I. Shtablavyi[a]; Yu. Kulyk[a]; U. E. Klotz[b]; C. Leinenbach[b]
[a] Department of Metal Physics, Ivan Franko National University, Lviv, Ukraine [b] EMPA - Swiss Federal Laboratories for Materials Testing and Research, Laboratory of Joining & Interface Technology, Duebendorf, Switzerland

To cite this Article Mudry, S. , Korolyshyn, A. , Shtablavyi, I. , Kulyk, Yu. , Klotz, U. E. and Leinenbach, C.(2009) 'The structure changes in $Sn_{1-x}Ti_x$ alloys at transition from liquid to solid state', Physics and Chemistry of Liquids, 47: 4, 437 — 446
To link to this Article: DOI: 10.1080/00319100802104863
URL: http://dx.doi.org/10.1080/00319100802104863

Physics and Chemistry of Liquids
Vol. 47, No. 4, August 2009, 437–446

Taylor & Francis
Taylor & Francis Group

The structure changes in $Sn_{1-x}Ti_x$ alloys at transition from liquid to solid state

S. Mudry[a]*, A. Korolyshyn[a], I. Shtablavyi[a], Yu. Kulyk[a], U.E. Klotz[b†] and C. Leinenbach[b]

[a]*Department of Metal Physics, Ivan Franko National University, Lviv, Ukraine;* [b]*EMPA – Swiss Federal Laboratories for Materials Testing and Research, Laboratory of Joining & Interface Technology, Duebendorf, Switzerland*

(*Received 22 January 2008; final version received 4 April 2008*)

The structures of $Sn_{1-x}Ti_x$ ($x = 0.00$; 0.02, 0.05, 0.15, 0.25; 0.35; 0.45) alloys were studied by X-ray diffraction at different temperatures. The structure factors, pair correlation functions, and parameters obtained were analysed. It is shown that the structures of the liquid alloys are inhomogeneous in the pre-crystallisation temperature region. The solidified phases are in agreement with the equilibrium phase diagram. The X-ray diffraction data were used for the specification of the liquidus line position.

Keywords: tin-based melts; brazing; phase diagram

1. Introduction

Binary Sn–Ti alloys form an important subsystem of the ternary Sn–Ti–Zr, as well as of the quaternary Cu–Sn–Ti–Zr system, which are of technical importance for active brazing filler metals [1,2]. These filler metals are used, for example, for brazing diamonds or cBN. High performance abrasive tools with chemically bonded diamond grit revealed a high bonding strength and an improved erosion resistance. The development of materials with predicted properties require a detailed knowledge of thermophysical and structure-sensitive properties of the alloys, especially in the melting–solidification temperature range. Several studies were dedicated to the Sn–Ti alloys, whereby most of them focus on the Sn-rich side of this system. A comprehensive review and assessment for the Sn–Ti binary system was reported by Murray [3] and recently by Liu *et al.* as well as Yin *et al.* [4,5]. A complete assessment of the binary and ternary subsystems of the Cu–Sn–Ti–Zr is described by Liu [6], expressing the need for further experimental data about the Cu–Sn–Ti–Zr system. In Figure 1, the most recent binary phase diagram calculated from the thermodynamic description of Liu [6] is presented.

The components of the Sn–Ti system reveal a substantial difference in their melting temperatures [6]. Therefore, the addition of a refractory element leads to a drastic increase of the liquidus temperature, and even a negligible error in the alloy composition can provoke a

*Corresponding author. Email: mudry@physics.wups.lviv.ua
†Present address: FEM, Research Institute for Precious Metals & Metals Chemistry, Schwaebisch, Gmuend, Germany.

ISSN 0031–9104 print/ISSN 1029–0451 online

DOI: 10.1080/00319100802104863
http://www.informaworld.com

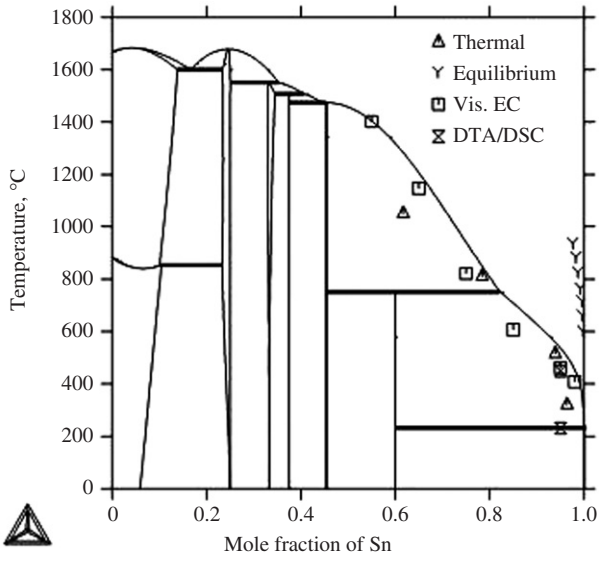

Figure 1. Equilibrium phase diagram of Sn–Ti system according to calculation of Liu [6], with comparison of the different experimental liquidus according to different methods [7,9,10].

serious error in the determination of the solidification onset. Because of this peculiarity and the experimental difficulties, the data on structure-sensitive properties of the system, as well as on its liquidus line are scarce and partly contradictory on the Sn-rich side [7–10]. Determination of the liquidus temperature by DTA methods is often very complicated and can lead to substantial errors. At this point, investigations by other methods, supplementing each other, enables this determination to a higher degree of accuracy.

In some recent studies of the liquid binary Sn–Ti alloys with a high Sn content (from 75 to 100 at.%), it was found that the Ti admixture influences variously the structure-sensitive properties of the liquid Sn, namely a reduced electrical conductivity and a substantial increase of the viscosity [10]. In this work, the structural changes at the liquidus–solidus transition of some binary Sn–Ti alloys on the Sn-rich side were studied by X-ray diffraction.

2. Experimental

Samples of $Sn_{1-x}Ti_x$ ($x = 0.00$; 0.02; 0.05; 0.15; 0.25; 0.35; 0.45) were prepared in an arc melting furnace in argon atmosphere and checked by X-ray micro-analysis. Ingots of tin (99.99% purity) and titanium (99.99% purity) were cleaned by chemical etching from oxide films, then mixed and installed in the chamber of the furnace. In order to achieve a good homogeneity, the alloys were re-melted 5 times, overheating by 50 K above the liquidus line. The temperature has been measured by means of a thermocouple, installed at the bottom part of the sample.

The diffraction studies were carried out using a high-temperature diffractometer with a special attachment that allows investigation of the solid and liquid samples at different temperatures up to 2000 K. Cu–K_α radiation monochromatised by means of a LiF single crystal as a monochromator and Bragg–Brentano focusing geometry were used.

The scattered intensities as a function of the scattering angle were recorded within the range $1\,\text{Å}^{-1} < k < 7\,\text{Å}^{-1}$, with different angular steps, which were equal to 0.05° within the region of the principal peak and 0.5° at the rest of the values of wave vectors. The scattered intensity was measured with high accuracy: better than 2%. In order to obtain the scattered intensities of such accuracy, the scan time was selected to be 100 s. Cu–K_α was used in order to have a higher resolution in the diffraction pattern. The error caused by the low value of the upper limit in Fourier transformation was estimated by Hoseman method [11]. The diffracted intensity was recorded using a NaI(Tl) scintillated detector in conjunction with an amplification system. The sample was placed in a rounded cup of 20 mm diameter. The X-ray diffraction measurements have been carried out in purified helium atmosphere.

Each sample was measured at three temperatures. The initial temperature of about 5 K above the corresponding liquidus temperature for each composition was determined earlier from electrical conductivity and viscosity data [10]. The second temperature was 10 K lower, and the third measurement was done at room temperature. The samples were maintained 30 min at each temperature.

The scattered intensities as functions of the scattering angles were recorded and corrected on absorption, anomalous dispersion and incoherent scattering [12].

The structure factors (SF) were obtained from angular dependences of scattered intensities. Pair correlation functions (PCF) were calculated from SF by means of Fourier-transformation.

$$g(r) = 1 + \frac{1}{2\pi^2 \rho_0 r} \int_0^\infty k[S(k) - 1] \sin(kr) \mathrm{d}k, \tag{1}$$

where k is the wave vector ($k = 4\pi(\sin\Theta/\lambda)$), $S(k)$ is the structure factor, ρ_0 is the mean atomic density, and γ is an interatomic distance. The density of molten alloys was calculated from X-ray data according to the procedures of [13,14].

From these functions the main structure parameters, namely the first and the second peak positions k_1, k_2, r_1, r_2, and a first peak height, $S(k_1)$, were determined. The number of neighbours, Z, was determined by symmetrical resolution on the principal peak of $4\pi r^2 \rho(r)$ function with an accuracy ±0.1.

In order to interpret the structure parameters obtained from the PCF, the model analysis was used. The model for a quasieutectic atomic distribution on the base Sn_n and Ti_n atomic groups and a random atomic distribution were used. The values of the most probable interatomic distances were calculated according to equations in [15,16]:

$$r_1^{S.A.} = x_{Sn} K_{Sn}^2 r_1^{Sn} + x_{Ti} K_{Ti}^2 r_1^{Ti}, \tag{2}$$

$$r_1^{R.D.} = (x_{Sn} K_{Sn} + x_{Ti} K_{Ti})^2 \left(x_{Sn} r_1^{Sn} + x_{Ti} r_1^{Ti}\right), \tag{3}$$

were r_1^{Sn}, r_1^{Ti} are the most probable interatomic distances for tin and titanium, K_{Sn}, K_{Ti}, x_{Sn}, x_{Ti} are the scattering abilities and atomic fractions of components, respectively.

3. Results

The SF for liquid $Sn_{0.98}Ti_{0.02}$ alloy, as shown in Figure 2(a), is similar to the SF of the liquid tin. Nevertheless, comparing the main parameters $-k_1$, k_2 as the first and second

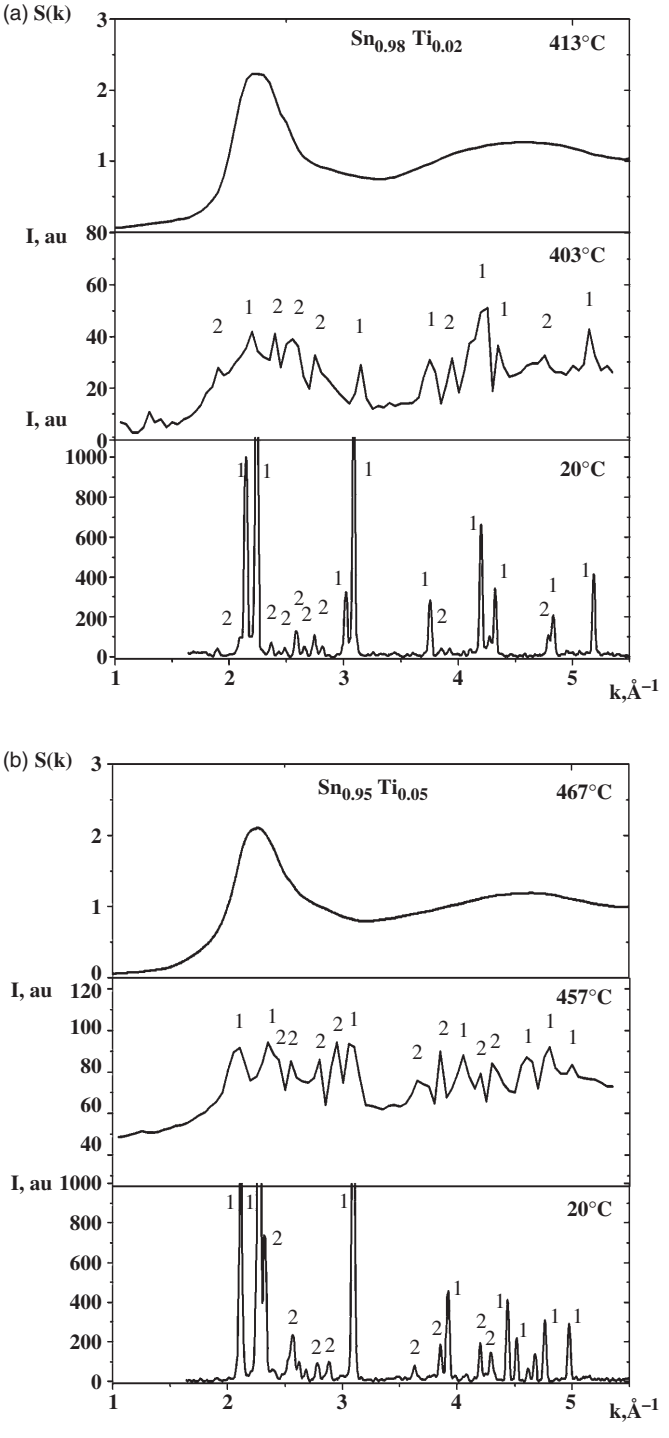

Figure 2. Structural changes at crystallisation for different $Sn_{1-x}Ti_x$ compositions: the upper curves were obtained in the completely liquid state; the curves in the middle were obtained just below the liquidus line; the lower curves were obtained at room temperature (1 – Sn; 2 – Ti_2Sn_3).

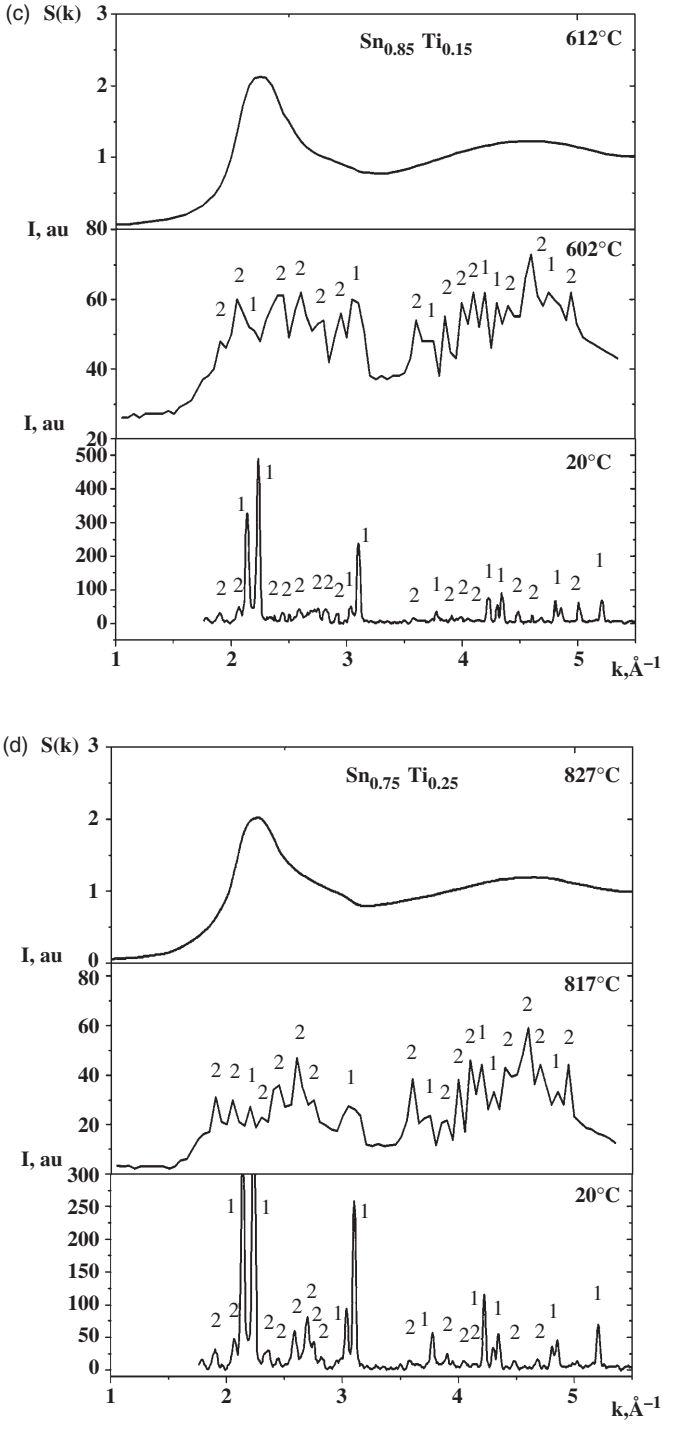

Figure 2. Continued.

Table 1. Structure parameters for $Sn_{1-x}Ti_x$ binary melts.

$Sn_{1-x}Ti_x$							
x	T (°C)	k_1Å^{-1}	k_2Å^{-1}	$S(k_1)$	r_1Å	r_2Å	Z
0.02	413	2.24	4.58	2.22	3.17	6.29	9.5
0.05	467	2.26	4.64	2.01	3.13	6.15	9.2
0.15	612	2.26	4.60	2.11	3.15	6.22	9.6
0.25	827	2.27	4.62	2.07	3.13	6.19	9.6
Sn	232	2.21	4.35	2.28	3.23	6.30	10.9
Ti	1700	2.45	4.41	2.38	3.17	6.00	10.9

Notes: T is a temperature 5 K above the melting point; k_1 is a first peak position of structure factor; k_2 is a second peak position of structure factor; $S(k_1)$ is a height of principal peak of structure factor; r_1, r_2 are the most probable interatomic distances and Z is a number of neighbours.

maxima positions, as well as $S(k_1)$, the principal peak height, reveals some discrepancies between them (Table 1). Similar features were observed for the PCF. Particularly, the most probable interatomic distances significantly reduce in comparison with the liquid tin. Accounting for this feature, one can suppose that liquid $Sn_{0.98}Ti_{0.02}$ alloy is not a simple solution with random atomic distribution. Although the content of Ti is small, its influence on the structure is considerable.

At cooling, the diffraction patterns reveal the appearance of peaks corresponding to the crystalline phases. The density of Ti_2Sn_3 crystallites is lower than that of the liquid alloy. Therefore, they swim up on the surface of the melt. Consequently, the temperature at which the crystalline-like peaks appear on the background of the diffraction pattern for the liquid phase can be considered as being close to the liquidus temperature. Peaks corresponding to crystalline phases are very wide due to a small crystallite size. The identification of the peaks, which are more clear at lower temperatures (cf. Figure 2(a)), allowed us to reveal the coexistence of solid Sn and Ti_2Sn_3 phases, which is in accordance with the available phase diagram.

The SF for molten $Sn_{0.95}Ti_{0.05}$ alloy also has the profile, which is close to the SF for the liquid tin (Figure 2(b)). In comparison with $Sn_{0.98}Ti_{0.02}$, the principal peak position is slightly shifted to larger k-values. A significant decrease of the height of the principal peak and of the distance to first neighbours confirms the intensive influence of Ti-atoms on atomic distribution of the tin structure. At a temperature of 457°C, the crystalline-like peaks appear on the background of the diffraction pattern for the liquid phase. As in the case of the $Sn_{0.98}Ti_{0.02}$ alloy, a further decrease in temperature promotes the aggregation of small crystallites, resulting in a diffraction pattern with narrow and sharp peaks. These peaks correspond to the same phases as in the previous alloy, namely Sn and Ti_2Sn_3.

Upon addition of Ti atoms up to 15 at.%, the changes in the structure become less pronounced than within a previous range of concentration. The SF of the melt containing 15 at.% Ti appear to be very similar to those of $Sn_{0.95}Ti_{0.05}$ (cf. Figure 2(c)). The same tendency for the formation of small crystallites (i.e. large clusters), which later increase their size by aggregation, is observed upon cooling.

A small shift of the principal and second peaks to the large k-values is observed comparing the SFs for liquid alloys containing 15 and 25 at.% Ti. The most probable interatomic distances have the same value (3.13 Å), which is less than those of the

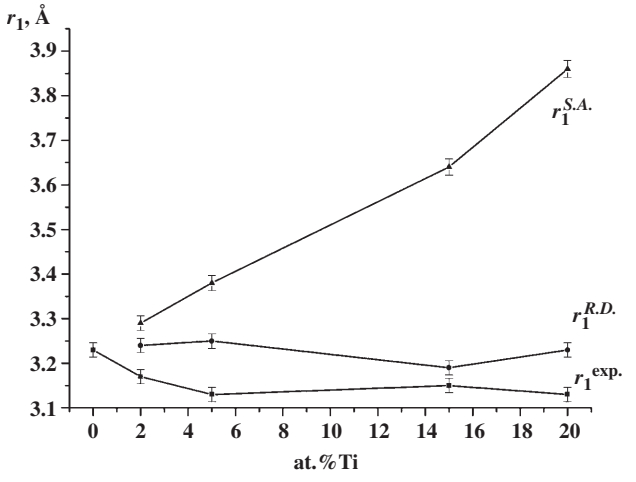

Figure 3. Results of model interpretation of the structure data ($r_1{}^{S.A.}$ – self-associated model; $r_1{}^{R.D.}$ – random atomic distribution; $r_1{}^{exp.}$ – experiment).

individual components Ti [17] and Sn, respectively (cf. Figure 2(d)). Such a decrease of the r_1 parameter is evidence for the increase of the interatomic interaction.

In this case, crystallisation starts at a temperature of 818°C. This value is in accordance with the temperature obtained from the physical property measurements [8].

It can be seen from the Table 1 that the number of neighbours, Z, is less for liquid Ti and Sn. The reason for such a difference is supposed to be caused by partial localisation of electrons, resulting in some covalent bonding between the atoms. This type of chemical ordering decreases the atomic packing density, which is observed in a reduction of Z.

The analysis of structure data was also carried out with the model method [10,15]. The models of the random atomic distribution and self-associated atomic arrangement, as mentioned above, were used. According to these models the most probable interatomic distances, $r_1^{S.A}$. and $r_1^{S.D}$, were calculated and compared with the experimental ones (Figure 3). As can be seen, the model of the random atomic distribution is in better agreement with the experimental data. The discrepancy between the model and the experimental values is supposed to be caused by structural inhomogeneities.

Alloys with a higher content of Ti (35 and 45 at.%) were studied at temperatures at which the formation of liquid tin and small crystallites of intermetallics – according to the peritectic reaction ($L + Ti_6Sn_5 \leftrightarrow Ti_2Sn_3$) – was observed.

It can be seen in Figure 4 that at $T = 1200$°C, a mixture of the liquid and crystalline phase exists. With further cooling, the fraction of each phase changes according to the phase diagram. The temperature interval where the liquid and crystalline phases coexist is large, and it should be noted that the size of the crystallites is small. Only upon cooling to lower temperatures does the formation of the complete solid state occur. The analysis of the diffraction patterns at $T = 20$°C reveals the existence of Sn, Ti_2Sn_3 and Ti_6Sn_5 phases. The solidified $Ti_{35}Sn_{65}$ alloy shows peaks which belong to the Sn, Ti_2Sn_3 and Ti_6Sn_5 phases. Here, it should be noted that the reflexes corresponding to Ti_6Sn_5 are significantly lower than the ones for the second phase. This is most probably caused by some deviation from the equilibrium cooling condition.

Similar behaviour is observed for the alloy containing 45 at.% Ti. The significant changes of the diffraction pattern occur with cooling. Upon crystallisation, Sn, Ti_2Sn_3 and

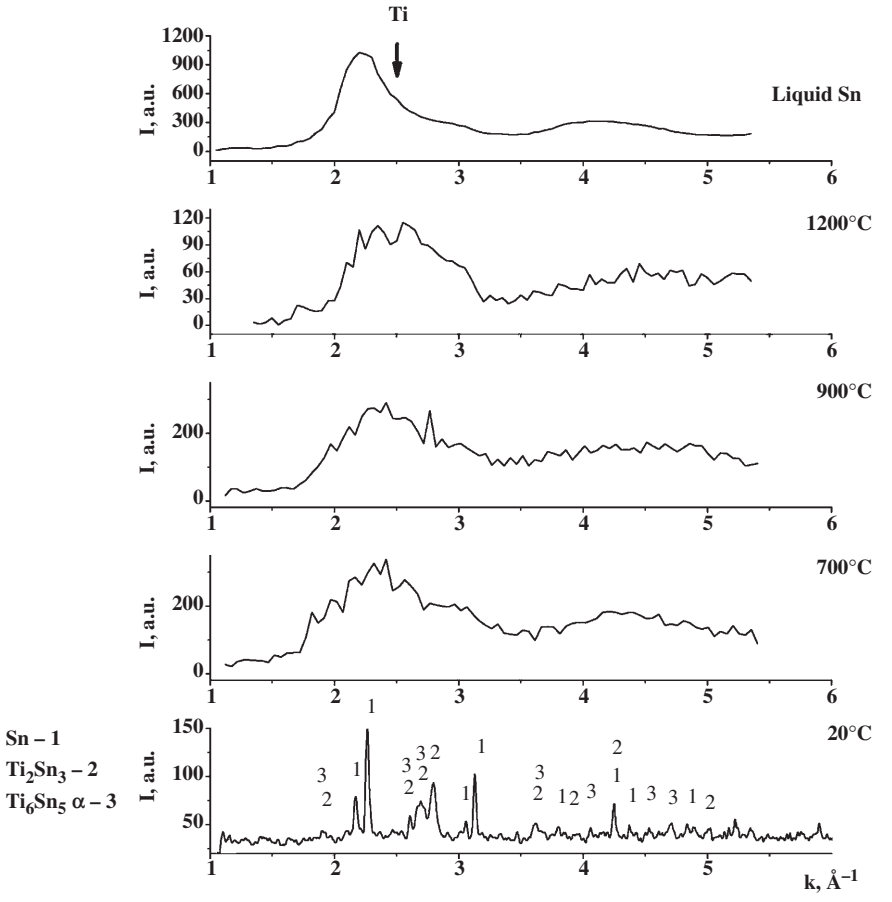

Figure 4. Structural changes at crystallisation for $Sn_{0.65}Ti_{0.35}$.

Ti_6Sn_5 α-phases exist, as well as the $Sn_{0.65}Ti_{0.35}$ sample (cf. Figure 5). It should be noted that the fraction of Ti_6Sn_5 α-phase is higher in $Sn_{0.65}Ti_{0.45}$, showing the accordance with the equilibrium phase diagram.

4. Discussion

Taking into account the results of the X-ray studies of liquid and solid $Sn_{1-x}Ti_x$ alloys, one can conclude that the influence of structural features of melts at the starting stage of crystallisation is significant. The alloys obviously tend to form chemically-ordered structural units with a structure similar to intermetallics. As a consequence, the existence of solid clusters in the liquid state is very likely. These clusters further agglomerate to larger structure units, which reach the critical size at the equilibrium conditions of crystallisation, and become the nuclei for the solid phase. Just before the solidification, a melt containing such clusters is supposed to be very sensitive towards outer influences (pressure, uncontrolled impurities, acoustic energy, electric and magnetic fields, etc.) and cooling conditions.

In some cases, the cluster aggregation process can be inhibited, resulting in undercooling. In further cases the opposite situation, when the cluster aggregation process

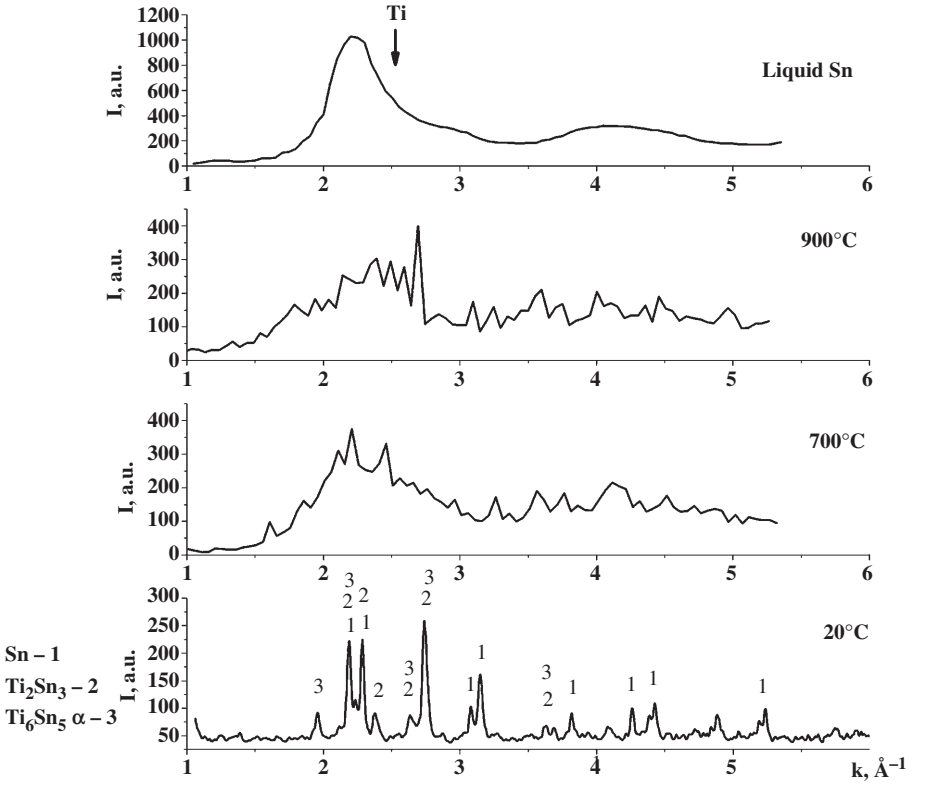

Figure 5. Structural changes at crystallisation for $Sn_{0.55}Ti_{0.45}$.

can be stimulated, is also possible, and the crystallisation process will start at a higher temperature than predicted by the equilibrium phase diagram.

5. Conclusions

The X-ray diffraction data show the inhomogeneous structure of $Sn_{1-x}Ti_x$ ($x = 0.02$; 0.05; 0.15; 0.25; 0.35; 0.45) molten alloys. The main structural units of these alloys are a matrix of tin and clusters of intermetallics. With cooling, the crystallisation process passes according to the equilibrium phase diagram. The liquidus temperatures for alloys containing 2, 5, 15 and 25 at.% Ti were found to be 408, 462, 607 and 822°C, respectively. Some discrepancies between these values and the ones obtained from other measurements can be attributed to different deviations from the equilibrium cooling condition.

References

[1] F.A. Khalid, U.E. Klotz, H.R. Elsener, B. Zigerlig, and P. Gasser, Scripta Mater. **50**, 1139 (2004).

[2] H.R. Elsener, U.E. Klotz, F.A. Khalid, D. Piazza, and M. Kiser, Adv. Eng. Mater. **7** (5), 375 (2005).

[3] J.L. Murray, in *Phase Diagrams of Binary Titanium Alloys*, edited by J.L. Murray (ASM International, Materials Park, OH, 1987), pp. 294–299.
[4] C. Liu, U.E. Klotz, P.J. Uggowitzer, and J.F. Löffler, Monatshefte für Chemie **136** (11), 1921 (2005).
[5] F. Yin, J.C. Tedenac, and F. Gascoin, CALPHAD **31**, 370 (2007).
[6] C. Liu, Ph. D. thesis, ETH Zurich No. 17469, 2007.
[7] V.N. Eremenko and T.Y. Velikanova, Russ. J. Inorg. Chem. **7**, 902 (1962).
[8] Ch. Kuper, W. Peng, A. Pisch, F. Goesmann, and R. Schmid-Feterzer, Z. Metallkd. **89**, 855 (1998).
[9] J.B. Darby and D.B. Jugle, T. Metall. Soc. AIME **245**, 2515 (1969).
[10] Yu. Plevachuk, S. Mudry, V. Sklyarchuk, A. Yakymovych, U.E. Klotz, and M. Roth, J. Mater. Sci. **42** (20), 8618 (2007).
[11] R. Hosemam, K. Lemm, and H. Krebs, Z. Phys. Chem. **41**, 121 (1964).
[12] A. Ilinskii, I. Kaban, and W. Hoyer, J. Non-Cryst. Solids. **347**, 39 (2004).
[13] W. Wang, X. Bian, and J. Qin, J. Mater. Sci. Lett. **19**, 1583 (2000).
[14] L.I. Mirkin, *Handbook on X-ray Structure Analysis* (Moscow, 1961) (in Russian).
[15] J.P. Hansen and I.R. McDonald, *Theory of Simple Liquids* (Academic Press, London, 1986).
[16] P.A. Egelstaff, *An Introduction to the Liquid State* (Oxford University Press, Oxford, 1992).
[17] Y. Waseda, (McGraw-Hill, New York, 1980). <http://www.tagen.tohoku.ac.jp/general/building/iamp/database/scm/>.